



Spontaneous imbibition characteristics of shale oil reservoir under the influence of osmosis

Yuliang Su^{1,2} · Qinghao Sun^{1,2} · Wendong Wang^{1,2} · Xincheng Guo^{1,2} · Jilong Xu^{1,2} · Guanqun Li^{1,2} · Xiugang Pu³ · Wenzhong Han³ · Zhannan Shi³

Received: 16 April 2022 / Accepted: 23 August 2022
© The Author(s) 2022

Abstract

The spontaneous imbibition (SI) process in shale oil reservoirs is not only influenced by capillary force, but also by the osmotic pressure between the fracturing fluid and formation water in the nanopores media. In this study, experimental methods are used to investigate the mechanisms of osmosis in the SI, taking into account the presence of initial formation water in shale oil reservoirs. To investigate the effect of osmosis, SI experiments were performed on the fine-grained felsic shale of the Qikou sag of Dagang oilfield. Low-field NMR testers and high-precision electronic balances are utilized for the measuring of oil–water migration. The results show that, when $S_w \neq 0$, high-salinity fluid SI can be divided into four stages: initial imbibition stage, drainage stage, secondary imbibition stage and stationary stage; when $S_w = 0$, there is no drainage stage of high-salinity fluid SI; when $S_w \neq 0$ or $S_w = 0$, low-salinity fluid SI can be called the “osmosis-enhanced SI”; and we have found that “newly formed pores or microfractures” as well as reducing salinity can promote SI. This article presents a systematic study of SI of shale oil reservoirs under the influence of osmosis, which provide useful information for reservoir numerical simulation and development program design.

Keywords Shale oil · Spontaneous imbibition · Osmosis · Water saturation · Capillarity

1 Introduction

According to a general definition, “shale oil” refers to liquid hydrocarbons and a variety of organic components found in organic-rich shale in different forms. The unique feature of the reservoir is its low porosity, low permeability and high organic content (Zhao et al. 2020), which is known to generate no natural industrial productivity and is subject to massive hydraulic fracturing (Sharifi et al. 2021). The flowback rate of fracturing fluid is very low, indicating that a large quantity of fracturing fluid has been trapped in the reservoir (King 2012; Singh 2016; Teklu et al. 2018). The traditional

view is that fluid retention during hydraulic fracturing leads to water blockage and clay swelling, which is detrimental to the recovery of crude oil from shale formations (Bazin et al. 2010; Bostrom et al. 2014; You et al. 2019; Yuliang et al. 2021). Field tests have indicated that some wells with low fracturing fluid flowback rates have been more productive than their nearby counterparts (Ghanbari and Dehghanpour 2016; Soleiman Asl et al. 2019). During the soaking process, spontaneous imbibition of the fracturing fluid reduces the flowback of the fluid (Ghanbari and Dehghanpour 2015; Haluszczak et al. 2013). The research into SI mechanisms of fracturing fluid has gradually become one of the hottest topics in the fracturing industry over the last few years, in an effort to improve the recovery of shale oil.

It has long been recognized that spontaneous imbibition (SI) is the process by which wettable fluid displaces non-wettable fluid out of pores in a matrix without external pressure, and capillary force is responsible for this process (Handy 1960; Takahashi and Kovscek 2010; Zhou et al. 2002). Since the inorganic pores in shale are largely hydrophilic surfaces (Pan et al. 2020; Yuan et al. 2021), water can penetrate into the pores through capillary action, displacing

✉ Wendong Wang
wwdong@upc.edu.cn

¹ Key Laboratory of Unconventional Oil & Gas Development, China University of Petroleum (East China), Ministry of Education, Qingdao 266580, China

² School of Petroleum Engineering, China University of Petroleum (East China), Qingdao 266580, China

³ PetroChina Dagang Oilfield Company, Tianjin 300280, China

oil (Gao et al. 2018; Sang et al. 2018). Aside from capillary force, osmotic pressure also plays an important role in imbibing fracturing fluid into shale reservoirs (Fakcharoenphol et al. 2014; Pan et al. 2021; Singh 2016). Osmosis refers to the phenomenon that two solutions of different concentrations are separated by a semi-permeable membrane, through which water molecules enter a high concentration solution from a low concentration solution, and the force that moves the water molecules is osmotic pressure (Fritz 1986; Hu et al. 2020).

In petroleum engineering, early studies on osmosis were conducted to solve wellbore stability problems encountered in drilling high-salinity shale formations (Mese 1995; Mody and Hale 1993; van Oort 1994). As a result of the U.S. shale oil and gas revolution, osmosis has gained new attention as a means of transporting fluids in porous shale reservoirs. According to some researchers, fracturing fluid composition has an impact on the ability of fracturing fluids to enter shale reservoirs (Hassan et al. 2012; Zheng and Sharma 2020). Karimi and Kazemi (2018) conducted SI experiments using a high-speed centrifuge under different salinity conditions to investigate how oil recovery differed with salinity brine. Ge et al. (2015) found that KCl solution in the concentration of 10 wt% can inhibit clay absorption to reduce the imbibition capacity of a shale gas reservoir, indirectly confirming the existence of chemical potential in shale. Padin et al. (2018) have shown that in shale gas reservoirs, water imbibition cannot be accounted for by capillary force alone, and osmosis is a major driving force for water transport. In addition, it is believed that in oil-wet shale reservoirs, low-salinity brine penetrates the matrix primarily through osmosis rather than capillary action (Bui and Tutuncu 2017; Torcuk et al. 2019). Zhou et al. (2016) studied the imbibition of high-salinity fluid into shale gas formation, finding that the SI process was governed by capillarity and osmosis.

Shale contains a lot of clay (Zhao et al. 2021), which is considered as a semi-permeable membrane because of its double electric structure (Fritz 1986; Greenberg et al. 1973; Keijzer and Loch 2001; Olsen 1972). In original conditions, besides clay, there is formation water in the shale oil reservoirs (Korb et al. 2014; Kurtoglu 2007; Li et al. 2016a; Xu

et al. 2022). During SI, water molecules can move through semi-permeable membranes (clay structure) because of the salinity difference between initial formation water and fracturing fluid (King 2012; Li et al. 2016b; Wang and Pan 2016; Zhou et al. 2021). However, formation water in shale oil reservoir is less and only exists in some inorganic pores (Gao et al. 2020; Hu et al. 2019; Wang et al. 2019), resulting in its neglect in SI experiments.

Most studies of shale SI involving osmosis focus on the effects of osmotic pressure on production, but few examine the full influence mechanism of osmosis and capillarity during imbibition. Additionally, most experimental investigations on osmosis in SI processes focus primarily on the external water phase inhalation process, rather than the water–oil phase replacement process. Also, the previous SI experiments of shale oil reservoir do not consider the existence of initial formation water in pores. Our goal in this study is to develop an SI experimental method for a shale oil reservoir based on NMR (nuclear magnetic resonance) testing and balance measurement where we consider the presence of initial formation water, and then study the osmosis mechanism in SI.

2 Shale samples

2.1 Petrophysical properties of samples

The samples of shale were collected from the Shahejie Formation in Qikou Sag, Dagang Oilfield, which lies at a depth of 4377.07 to 4378.40 m. The lithology was fine-grained felsic sedimentary rock. Except for length and weight of the shale samples, the physical properties (Table 1) are basically the same.

2.2 X-ray diffraction (XRD) analysis

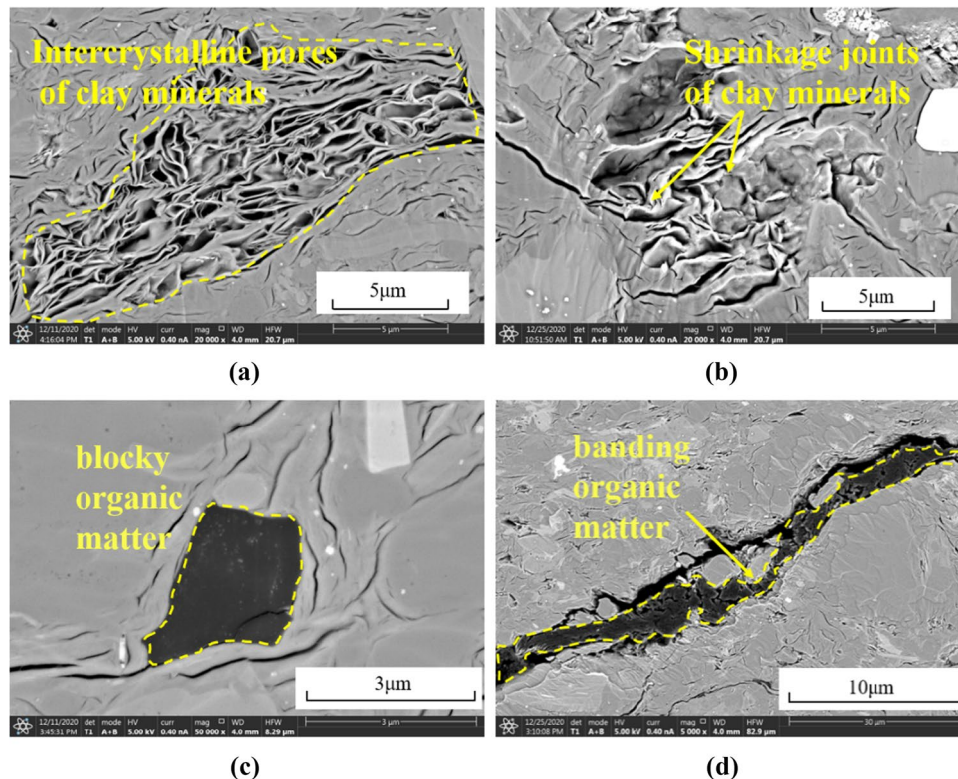
Minerals in the samples were investigated using XRD technology. The mineralogical composition of the studied samples is shown in Table 2. Shale samples are mainly composed of quartz, followed by dolomite and calcite with

Table 1 Physical properties of shale samples

Sample	Diameter (cm)	Length (cm)	Weight (g)	Porosity (%)	Permeability (mD)
B1	2.402	2.726	31.715	7.59	0.00175
B2	2.402	2.332	27.141	7.59	0.00175
F	2.385	4.883	55.634	5.20	0.00214
L	2.380	5.399	61.733	4.53	0.00278
N	2.388	5.412	62.874	4.11	0.00196
X	2.400	2.580	30.012	4.45	0.00132
Y1	2.400	2.570	29.417	6.29	0.00147
Y2	2.400	2.082	24.165	6.29	0.00147

Table 2 Mineralogical composition and mass fraction of shale samples (%)

Sample	Quartz	Dolomite	Calcite	Feldspar	Analcime	Siderite	Pyrite	Kaolinite	Illite	Smectite
B1 & B2	47.83	19.64	13.86	2.12	1.79	0.04	0.45	5.78	6.15	2.34
F	56.29	12.78	14.73	2.02	1.84	0	0.29	5.85	4.76	1.46
L	50.43	17.22	13.27	2.09	1.77	0	0.29	6.36	6.22	2.34
N	56.15	16.50	9.46	2.43	2.07	0	0.27	5.39	5.33	2.39
X	54.25	16.76	10.36	2.60	2.20	0	0.26	5.60	5.78	2.20
Y1&Y2	49.72	17.27	13.54	2.15	2.20	0	0.39	6.60	5.65	2.48

**Fig. 1** Scanning electron microscope images

average contents of approximately 52.45 wt%, 16.70 wt% and 12.54 wt%, respectively. The dominate clay minerals are kaolinite, followed by illite with average contents of 5.93 wt% and 5.65 wt%, respectively.

2.3 SEM and N₂ adsorption analysis

The samples contain a majority of inorganic intercrystalline pores (Fig. 1a), as well as inorganic intragranular pores and clay mineral shrinkage joints (Fig. 1b). In addition, the samples contain low levels of organic matter, nanopores in organic matter are typically underdeveloped (Fig. 1c), and organic pores are visualized only locally (Fig. 1d).

We conducted a low-temperature nitrogen adsorption (LTNA) experiment on shale sample F and L. The

low-temperature N₂ adsorption–desorption isotherms shows an inverse “S” shape (Fig. 2), which is characteristic of the type IV isotherm, and implies that the samples contain mesopores or macropores besides micropores. In addition, Table 3 provides the pore structure parameters of the samples, which are calculated according to the BJH (Barret-Joyner-Halenda) theory and the BET (Brunauer–Emmett–Teller) theory.

2.4 Contact angle measurement

An investigation of the contact angle in the shale-oil–water system was conducted using sample L, and SL200KB is applied to measure the contact angle using optical projection method. The shale flakes have been polished, since the

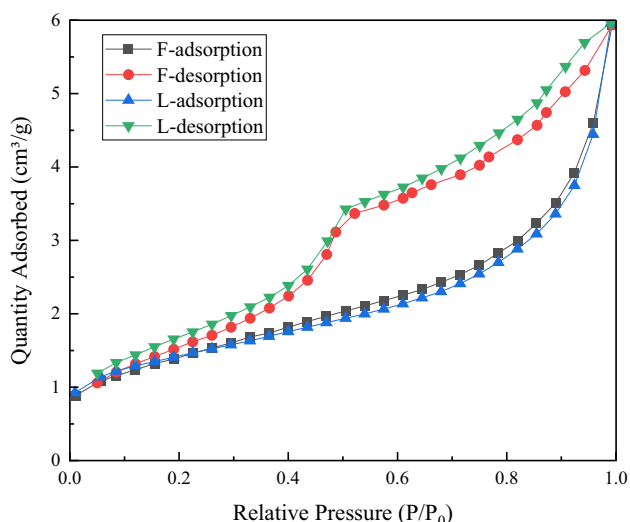


Fig. 2 Low-temperature N₂ adsorption–desorption isotherms of shale samples

real core surface is porous and cannot be tailored to the regular shape. As shown in Fig. 3, when the steady-state of the drop on the surface is reached, a tangent line is drawn to quantify the contact angle. According to the results of the experimental work, the water contact angle of the sample in the shale-oil–water system is about 37°, indicating that the shale sample is more hydrophilic in the reservoir environment where oil and water coexist.

3 Imbibition experiment

3.1 Experimental equipment

As shown in Fig. 4, the equipment used in the SI experiment consists of an electronic balance with an accuracy of 0.001 g, a beaker, a computer and a low-field NMR instrument. During the experiment, the beaker should be sealed and shaded.

Fig. 4 Schematic diagram of SI experiment and NMR instrument

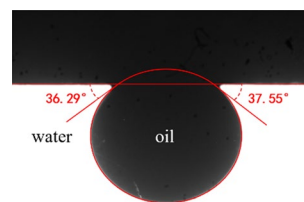
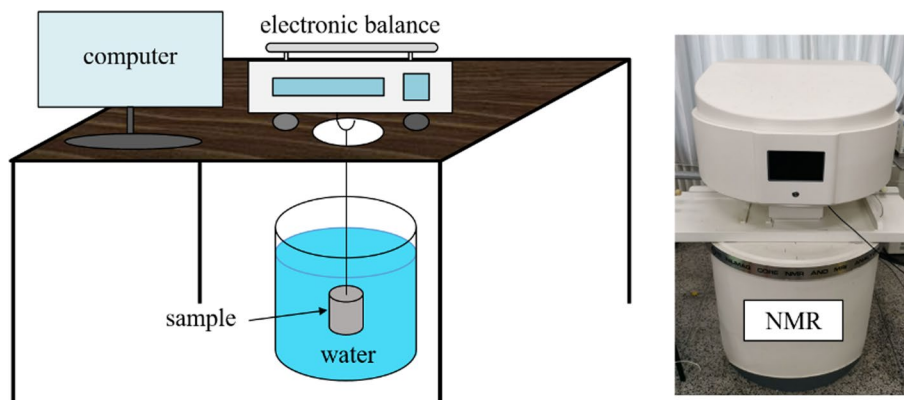


Fig. 3 Water contact angle in the shale-oil–water system

Table 3 Pore structure parameters of the samples

Sample	BJH cumulative volume of pores (cm ³ /g)		BJH average pore diameter (nm)		BET surface area (m ² /g)
	Adsorption	Desorption	Adsorption	Desorption	
F	0.008574	0.009215	8.7004	5.4609	5.0664
L	0.008361	0.009250	9.9631	5.2806	4.9680

3.2 Experimental procedure

There are four groups of experiments, and the core samples and imbibition working fluid are listed in Table 4. The specific experimental steps were as follows:

- (1) Configure the imbibition working fluid, the formula is shown in Table 4. Configure the formation water with salinity of 16,739 mg/L (1.67 wt%) CaCl₂.
- (2) After core cleaning, dry the shale core samples at 110 °C for 48 h. Measure the core size and dry weight, and perform an NMR T₂ spectra test.
- (3) Vacuumize the core and saturate it with 10% pore volume formation water. Then pressurize 30 MPa saturate shale oil, fully saturate for 20 days. Measure the wet weight of the core and test the core again with NMR T₂ spectra.

Table 4 Each group of samples corresponding to the imbibition working fluid

Experimental class	S_w (%)	Samples	Imbibition working fluid	Test method
① High-salinity fracturing fluid SI	10	F L	Slick water (0.1 wt% anti-swelling agent, 0.1 wt% drag reduction agent, 0.1 wt% KCl) + 18 wt% $MnCl_2 \cdot 4H_2O$	Electronic balance test, NMR test
② High-salinity brine SI	10	B2	24 wt% KCl solution	Electronic balance test
③ Low-salinity fracturing fluid SI	10	N	Slick water (0.1 wt% anti-swelling agent, 0.1 wt% drag reduction agent, 0.1 wt% KCl)	
④ Different salinities brine SI	0	B1	1 wt% KCl solution	
		Y1	8 wt% KCl solution	
		Y2	24 wt% KCl solution	
		X	Deionized water	

- (4) Hook the core from the bottom of the balance, and place it in a beaker filled with imbibition working fluid. Record the initial weight of the core after water entry, and then record it every 10 s. During imbibition, oil adhered to the core wall is removed with a fine needle tip.
- (5) After a time, take out the core and measure the NMR T_2 spectra, then repeat the experiment step (4). The experiment can be ended until the NMR T_2 spectra remains unchanged.

In addition, it should be noted that the experiment ④ in step (3) only saturated shale oil. Experiment ②, ③ and ④ cannot be carried out in step (5) because the imbibition working fluid cannot shield hydrogen nuclear signal in water. They can be terminated in step (4) when the core weight is constant.

4 Results and discussion

4.1 Imbibition recovery of fracturing fluid

As for experiment 1 in Table 4, NMR T_2 spectra were recorded during the SI of the fracturing fluid (slick water). NMR T_2 spectra were plotted as shown in Fig. 5 (after subtracting sample substrate signals). The T_2 spectrum exhibits three peaks. The area of the left peak is considerably larger than that of the other peaks, and the middle peak and the right peak are continuous. In the early stage of imbibition, T_2 spectra decreased rapidly, after imbibition for 268 h, the T_2 spectra were basically stable. The imbibition recovery ratio can be calculated by the T_2 spectrum area before and after imbibition. The calculation formula of imbibition recovery ratio is as follows:

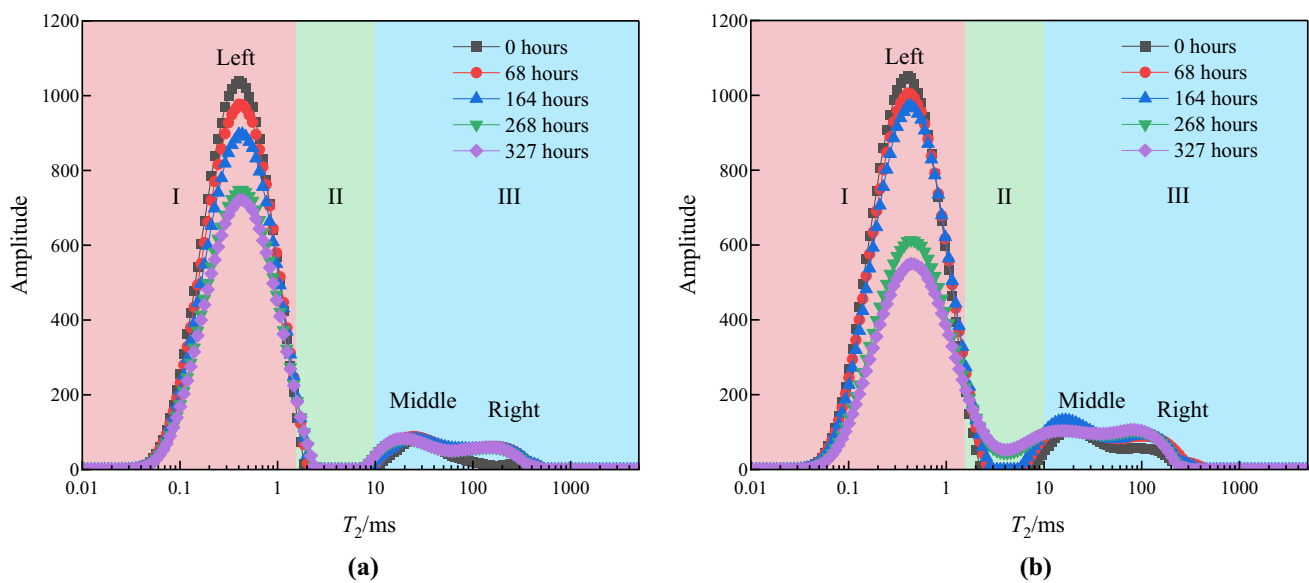


Fig. 5 NMR T_2 spectra of fracturing fluid SI: **a** Sample F; **b** Sample L

$$E = \frac{S_0 - S}{S_0} \quad (1)$$

where, E is the recovery ratio; S_0 is T_2 spectrum area before SI, and S is T_2 spectrum area after SI.

For region I in Fig. 5, we know that the main variation of the T_2 spectra is the left peak. It shows that smaller pores are more efficiently penetrated by fracturing fluid. The reason for this is that the smaller the size of shale pores, the greater the capillary force, the stronger the driving force of imbibition. For region III in Fig. 5, it is noted that the area of the middle peak and right peak in T_2 spectra does not change significantly. This is because the larger pores act primarily as migration channels during SI, and oil remains in the larger pores after SI (Li et al. 2019).

The shale oil recovery of F, and L was calculated based on the NMR T_2 spectra (Fig. 5). The imbibition recovery ratio of sample L is 32.18%, which is higher than 21.45% of sample F. The reason for this is that the “newly formed pores or microfractures” improve oil–water flow capacity. For region II in Fig. 5b, the left peak and middle peak of sample L were originally discontinuous, and the amplitude between them was zero. However, during imbibition, the amplitude of T_2 spectra in this section (1–10 ms range) increases significantly. This indicates the formation of new pores or microfractures, and that oil in smaller pores is replaced by water into this space, resulting in the detection of a NMR signal of oil there. By comparing the curves of L sample at 268 h and 164 h, it can be found that the area of the left peak (region I) decreases rapidly with the formation of new pores or microfractures. It shows that “newly formed pores or microfractures” can act as channel for oil migration, facilitating the replacement of oil in smaller pores.

4.2 Drainage of high-salinity fluid SI

In order to simulate the oil–water two-phase environment in the shale pores, as for experiment 1 in Table 4, the core was saturated with 10% PV formation water and then saturated with shale oil. In addition, 18 wt% $\text{MnCl}_2 \cdot 4\text{H}_2\text{O}$ was added to the imbibition working fluid, so that the experiment carried out is high-salinity (higher than formation water salinity) fracturing fluid SI experiment. Due to the density difference between water and oil, the slick water displaces the oil from the core causing the weight of the core to increase. To compare the imbibition results of different samples, we subtracted the initial weight from the real-time weight and then obtained the change in sample weight.

It can be seen from Fig. 6 that the weight of shale core generally increases. However, after a short period of growth (stage I), a decline stage appears (stage II). By changing the

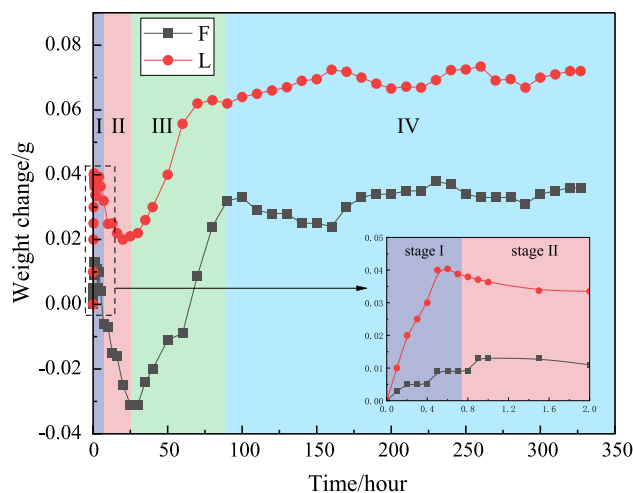


Fig. 6 SI of high-salinity slick water (18 wt% $\text{MnCl}_2 \cdot 4\text{H}_2\text{O}$), $S_w \neq 0$

type of imbibition working fluid, an SI experiment (experiment 2 in Table 4) of high-salinity (higher than formation water salinity) brine was conducted on B2 sample, which also shows decline stage (Fig. 7a). This phenomenon is consistent with Bin Pan’s observation of shale gas core with high-salinity brine SI experiment (Pan et al. 2021). On this basis, considering the water–oil two-phase, the mechanism of shale oil core may be more complex. In addition, when the core is completely saturated with oil ($S_w = 0$), and the high-salinity brine SI experiment (experiment 4 in Table 4) is carried out on Y2 sample, there is no decline stage (Fig. 7b). This indicates that only when $S_w \neq 0$, that is, there is formation water in the pores, the decline stage can occur in the high salinity fluid SI experiment.

The decrease of sample weight indicates fluid outflow from the core, which is caused by osmosis. Because there is a salinity difference between the high-salinity brine/slick water outside the sample and the formation water inside, and the clay in shale can act as a semi-permeable membrane. The salinity difference will provide an osmotic pressure for the fluid on either side of the semi-permeable membrane (Fig. 8). When the salinity of formation water in the pore is smaller than that of the fluid outside the pore, the water molecules in the pore and the clay structure will migrate to the outside of the pore under osmotic pressure (Fig. 9). This results in water outflow from the core. Therefore, stage II in Figs. 6 and 7a can be defined as the drainage stage to characterize the outflow of water. This theory can explain the anomalous phenomenon that often occurs in shale SI experiments based on NMR technology: the decrease of core weight. The addition of a large amount of $\text{MnCl}_2 \cdot 4\text{H}_2\text{O}$ makes the imbibition working fluid become a high-salinity fluid, resulting in drainage phenomenon in shale SI.

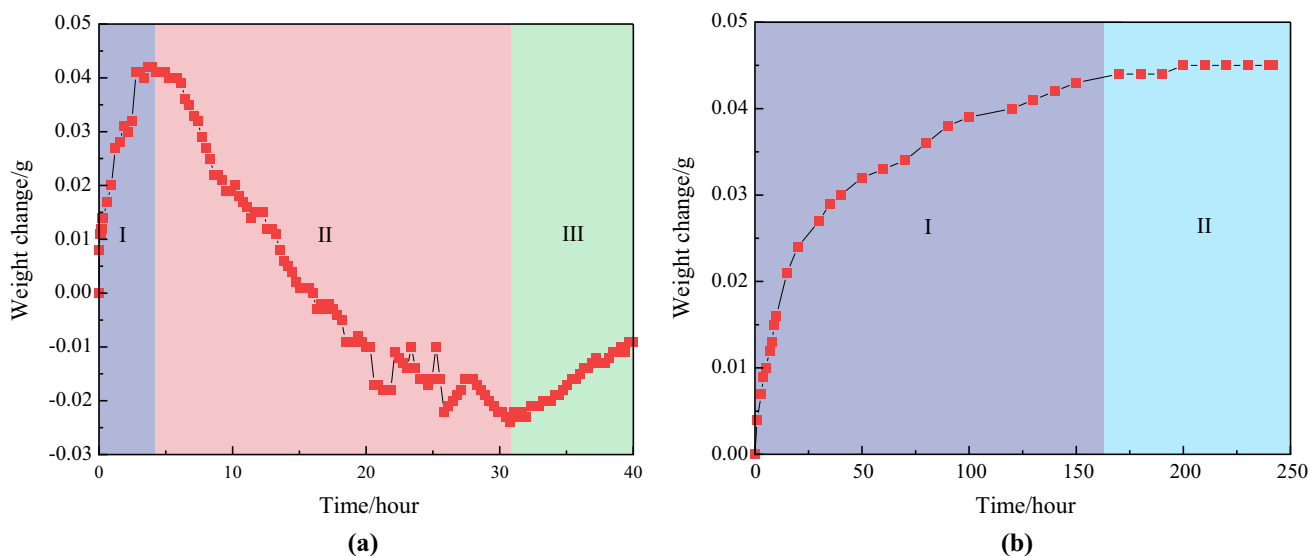


Fig. 7 SI of high-salinity brine (24 wt% KCl). a $S_w \neq 0$; b $S_w = 0$

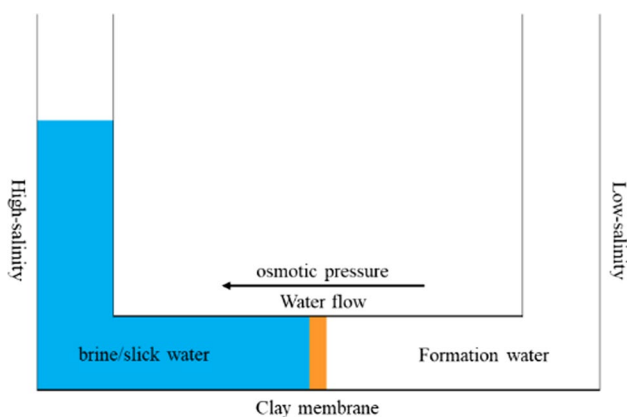


Fig. 8 Schematic diagram of osmotic pressure in high-salinity fluid SI

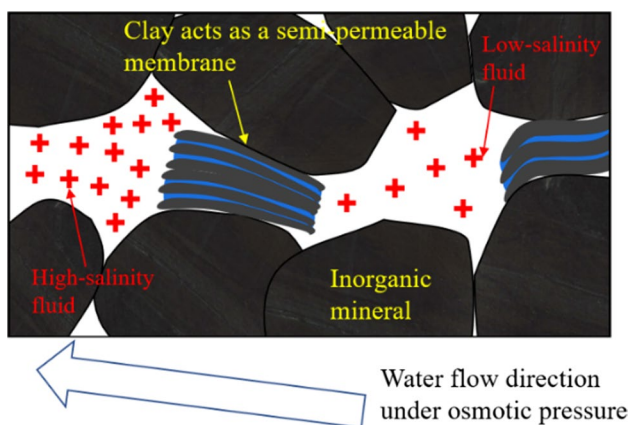


Fig. 9 Effect of osmotic pressure on external higher salinity fluids

According to Fig. 6, when $S_w \neq 0$, high-salinity fluid imbibition can be divided into four stages: initial imbibition stage (stage I), drainage stage (stage II), secondary imbibition stage (stage III) and stationary stage (stage IV). Osmotic pressure and capillary force play an important role in these four stages, and their magnitude changes constantly. Stage I, the initial imbibition stage, occurs after the sample is immersed in the imbibition working fluid and lasts for a short time. During this time, a small amount of high-salinity fluid enters the core under capillary force. Capillary force was weakened as the result of increasing water saturation. Stage II is the drainage stage when the osmotic pressure is stronger than the capillary force. Water molecules in clay structure and micro/nano pores enter high-salinity fluid under osmotic pressure. It should be noted that the weight increase during other stage is due to the density difference between water and oil, while the weight decrease is the weight of the lost fluid during drainage stage, so the weight change during drainage stage is more obvious. In the drainage stage, the capillary force increases with the decrease of S_w in the core. However, the osmotic pressure decreases with the increase of the salinity of the fluid in the core. When the capillary force exceeds the osmotic pressure enough to control imbibition, stage III, the secondary imbibition stage begins. This stage is similar to the initial imbibition stage, where high-salinity fluid further enters into shale pores under capillary force. In stage IV, a mass of high-salinity fluid has entered the core and a mass of shale oil has been displaced. During this stage, imbibition occurs very slowly until SI stops. In general, the drainage stage is dominated by osmosis, while the initial and secondary imbibition stages are dominated by capillarity.

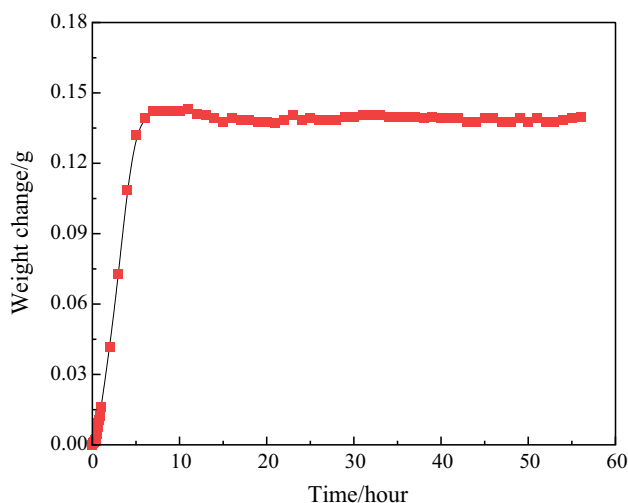


Fig. 10 SI of low-salinity slick water (0.1 wt% KCl), $S_w \neq 0$

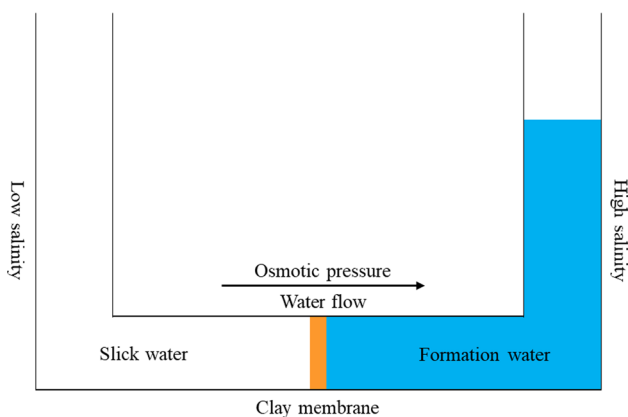


Fig. 11 Schematic diagram of osmotic pressure in low-salinity fluid SI

4.3 Osmosis-enhanced SI of low-salinity fluid

The salinity of fracturing fluid in oilfield is generally about 0.1%, which is less than that of formation water in shale (Haluszczak et al. 2013). SI experiment of low-salinity fracturing fluid (0.1 wt% KCl) was carried out (experiment 3 in Table 4) with the sample N ($S_w \neq 0$), and the core weight changes are shown in Fig. 10. It can be seen from Fig. 10 that no drainage stage occurs during the SI of low-salinity slick water, and the water inhaled is significantly more than that of high-salinity slick water SI shown in Fig. 6. In addition, the stationary stage of SI also appears in advance, which illustrates that low-salinity fluid SI also can increase the imbibition velocity.

The reason for this is that the salinity of the slick water outside the core is lower than that of the formation water inside the pore (Fig. 11), and osmotic pressure facilitates the water molecules enter shale pore. In addition, osmosis can assist capillarity in the displacement of oil by slick water. Figure 12 is a schematic diagram of osmosis mechanism in shale containing oil and water. Initially, oil occupies most of the pore space, and a small amount of formation water exists on the clay structure and some inorganic mineral surfaces (Fig. 12a). Under osmotic pressure, water molecules in low salinity solution can enter the clay structure and inorganic pores. As a result, pore pressure increases, and oil is expelled through the larger pores (Fig. 12b). In the actual formation, osmosis will facilitate fracturing fluid entry into shale, leading to faster and deeper SI, which can be called “osmosis-enhanced SI”. This also explains the low flowback ratio in shale formations.

SI experiment of different salinities brine (experiment 4 in Table 4) was carried out with the samples which are completely saturated with oil ($S_w = 0$), and the cores weight change is shown in Fig. 13. It can be find that the core weight changes of deionized water and 1 wt% KCl solution were significantly greater than that of 8 wt%/24 wt% KCl solution. It indicates

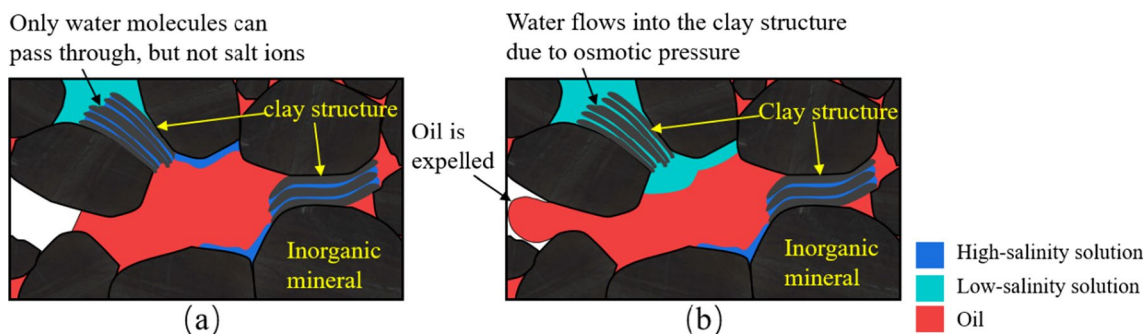


Fig. 12 Schematic diagram of osmosis mechanism in shale containing oil–water two-phase: a Pore space containing oil–water two-phase; b Water displaces the oil out of the pores

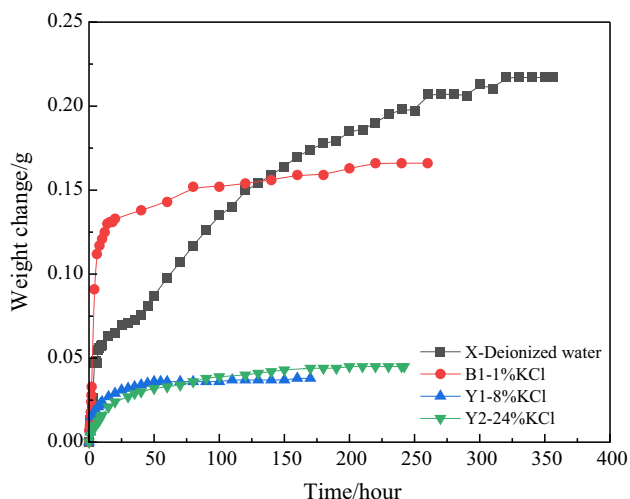


Fig. 13 SI of brine with different salinities, $S_w = 0$

that in the SI experiment of shale samples with S_w of 0, with the increase of S_w during imbibition, low-salinity fluid can still play the role of “osmosis-enhanced SI”.

Salinity determines the magnitude and direction of osmotic pressure. Combined with the theoretical osmotic pressure calculation formula proposed by Marine and Fritz (1981), the actual osmotic pressure on both sides of clay in shale can be described by the following formula:

$$P_\pi = \eta \frac{RT}{V} \ln \frac{A_{sh}}{A_f} \tag{2}$$

where P_π is osmotic pressure, η is membrane efficiency, V is partial molar volume of water ($1.8 \times 10^{-5} \text{ m}^3/\text{mol}$), R is gas constant, T is absolute temperature, A_{sh} and A_f is water activity on both sides of clay, which depending on the salinity of the fluid.

It can be seen from Fig. 13 that the imbibition amount of deionized water is higher than 1 wt% KCl solution. This is because, with the decrease of salinity, the water activity of brine increases. When the water activity of the fluid inside the pore is constant, the lower the salinity outside the pore, the greater the A_{sh} and the greater the osmotic pressure. Therefore, the effect of SI can be improved by reducing the salinity of brine/slick water.

5 Conclusions

In this paper, we developed an SI experimental methodology of shale oil reservoir considering the presence of initial formation water, and the osmosis mechanism in SI was studied in-depth. The following conclusions were drawn from the research:

- (1) New pores or microfractures are easily formed in shale during the SI of fracturing fluid, which can act as channel for oil migration, facilitating the replacement of shale oil in smaller pores.
- (2) When $S_w \neq 0$, High-salinity fluid SI can be divided into four stages: initial imbibition stage, drainage stage, secondary imbibition stage and stationary stage. The salinity difference between the external fluid and the formation water leads to the drainage stage, which is dominated by osmosis. The initial and secondary imbibition stages are dominated by capillarity. When $S_w = 0$, there is no drainage stage.
- (3) When $S_w \neq 0$, in low-salinity fluid SI, osmosis can promote the migration of external fluid into shale pores, and assist capillarity in the displacement of shale oil, which can be called “osmosis-enhanced SI”. When $S_w = 0$, with the increase of S_w during SI, low-salinity fluid can still play the role of “osmosis-enhanced SI”. In addition, reducing salinity of brine/slick water can promote SI.

Acknowledgements This study was funded by the National Natural Science Foundation of China (52274056, 51974348).

Declarations

Competing interest The authors declare that we have no known competing financial interests or personal relationships that could have appeared to influence the work reported in this paper.

Open Access This article is licensed under a Creative Commons Attribution 4.0 International License, which permits use, sharing, adaptation, distribution and reproduction in any medium or format, as long as you give appropriate credit to the original author(s) and the source, provide a link to the Creative Commons licence, and indicate if changes were made. The images or other third party material in this article are included in the article's Creative Commons licence, unless indicated otherwise in a credit line to the material. If material is not included in the article's Creative Commons licence and your intended use is not permitted by statutory regulation or exceeds the permitted use, you will need to obtain permission directly from the copyright holder. To view a copy of this licence, visit <http://creativecommons.org/licenses/by/4.0/>.

References

Bazin B et al (2010) In-situ water-blocking measurements and interpretation related to fracturing operations in tight gas reservoirs. *SPE Prod Oper* 25:431–437

Bostrom N et al (2014) The time-dependent permeability damage caused by fracture fluid. In: *SPE international symposium and exhibition on formation damage control*, pp D011S006R001

Bui BT, Tutuncu AN (2017) Contribution of osmotic transport on oil recovery from rock matrix in unconventional reservoirs. *J Petrol Sci Eng* 157:392–408

- Fakcharoenphol P, Kurtoglu B, Kazemi H, Charoenwongsa S and Wu Y-S (2014) The effect of osmotic pressure on improve oil recovery from fractured shale formations. In: SPE unconventional resources conference, pp D021S003R004
- Fritz SJ (1986) Ideality of clay membranes in osmotic processes: a review. *Clays Clay Miner* 34(2):214–223
- Gao L, Yang Z, Shi Y (2018) Experimental study on spontaneous imbibition characteristics of tight rocks. *Adv Geo-Energy Res* 2:292–304
- Gao Z, Fan Y, Xuan Q, Zheng G (2020) A review of shale pore structure evolution characteristics with increasing thermal maturities. *Adv Geo-Energy Res* 4:247–259
- Ge H-K et al (2015) Experimental investigation of shale imbibition capacity and the factors influencing loss of hydraulic fracturing fluids. *Pet Sci* 12(4):636–650
- Ghanbari E, Dehghanpour H (2015) Impact of rock fabric on water imbibition and salt diffusion in gas shales. *Int J Coal Geol* 138:55–67
- Ghanbari E, Dehghanpour H (2016) The fate of fracturing water: a field and simulation study. *Fuel* 163:282–294
- Greenberg JA, Mitchell JK, Witherspoon PA (1973) Coupled salt and water flows in a groundwater basin. *J Geophys Res* (1996–1977) 78(27):6341–6353
- Haluszczak LO, Rose AW, Kump LR (2013) Geochemical evaluation of flowback brine from Marcellus gas wells in Pennsylvania, USA. *Appl Geochem* 28:55–61
- Handy LL (1960) Determination of effective capillary pressures for porous media from imbibition data. *Trans AIME* 219(01):75–80
- Hassan D, Zubair H, Chhabra A, Ullah A (2012) Liquid intake of organic shales. *Energy Fuels* 26:5750–5758
- Hu Z et al (2019) Influence of reservoir primary water on shale gas occurrence and flow capacity. *Nat Gas Ind B* 6(1):71–78
- Hu Y et al (2020) Mechanisms of fracturing fluid spontaneous imbibition behavior in shale reservoir: a review. *J Nat Gas Sci Eng* 82:103498
- Karimi S, Kazemi H (2018) Characterizing pores and pore-scale flow properties in Middle Bakken Cores. *SPE J* 23(04):1343–1358
- Keijzer T, Loch G (2001) Chemical osmosis in compacted dredging sludge. *Soil Sci Soc Am J* 65:1045–1055
- King GE (2012) Hydraulic Fracturing 101: what every representative, environmentalist, regulator, reporter, investor, university researcher, neighbor and engineer should know about estimating frac risk and improving frac performance in unconventional gas and oil wells. In: SPE hydraulic fracturing technology conference
- Korb J-P, Nicot B, Louis-Joseph A, Bubicci S, Ferrante G (2014) Dynamics and wettability of oil and water in oil shales. *J Phys Chem C* 118:23212–23218
- Kurtoglu B (2007) Integrated reservoir characterization and modeling in support of enhanced oil recovery for Bakken. Colorado School of Mines, Colorado
- Li J et al (2016a) A quantitative model to determine water-saturation distribution characteristics inside shale inorganic pores. *Acta Pet Sin* 37(07):903–913
- Li C, Mao W, Wu T, Zhu S (2019) A study on mechanism of oil displacement by imbibition. *Xinjiang Pet Geol* 40(06):687–694
- Li X, Abass H, Teklu TW and Cui Q (2016b) A shale matrix imbibition model—interplay between capillary pressure and osmotic pressure. In: SPE annual technical conference and exhibition
- Marine IW, Fritz SJ (1981) Osmotic model to explain anomalous hydraulic heads. *Water Resour Res* 17(1):73–82
- Mese AI (1995) Effects of fluid saturation and stress state on the mechanical and chemical properties of shale. The University of Texas at Austin, Texas
- Mody FK, Hale AH (1993) Borehole-stability model to couple the mechanics and chemistry of drilling-fluid/shale interactions. *J Petrol Technol* 45(11):1093–1101
- Olsen HW (1972) Liquid movement through kaolinite under hydraulic, electric, and osmotic Gradients I. *AAPG Bull* 56(10):2022–2028
- Padin A, Torcuk M, Katsuki D, Kazemi H, Tutuncu A (2018) Experimental and theoretical study of water and solute transport in organic-rich carbonate mudrocks. *SPE J* 23:704–718
- Pan B, Yin X, Iglauer S (2020) A review on clay wettability: from experimental investigations to molecular dynamics simulations. *Adv Coll Interface Sci* 285:102266
- Pan B et al (2021) Fracturing fluid loss in unconventional reservoirs: evaluating the impact of osmotic pressure and surfactant and methods to upscale results. In: SPE/AAPG/SEG unconventional resources technology conference, pp D021S042R003
- Sang Q, Zhang S, Li Y, Dong M, Bryant S (2018) Determination of organic and inorganic hydrocarbon saturations and effective porosities in shale using vacuum-imbibition method. *Int J Coal Geol* 200:123–134
- Sharifi M, Kelkar M, Karkevandi-Talkhooncheh A (2021) A workflow for flow simulation in shale oil reservoirs: a case study in woodford shale. *Adv Geo-Energy Res* 5:365–375
- Singh H (2016) A critical review of water uptake by shales. *J Nat Gas Sci Eng* 34:751–766
- Soleiman Asl T, Habibi A, Ezulike OD, Eghbalvala M and Dehghanpour H (2019) The role of microemulsion and shut-in on well performance: from field scale to laboratory scale. In: SPE Hydraulic fracturing technology conference and exhibition
- Takahashi S, Kovscek A (2010) Spontaneous countercurrent imbibition and forced displacement characteristics of low-permeability, siliceous shale rocks. *J Pet Sci Eng* 71:47–55
- Teklu TW et al (2018) Low-salinity water and surfactants for hydraulic fracturing and EOR of shales. *J Pet Sci Eng* 162:367–377
- Torcuk MA, Uzun O, Padin A and Kazemi H (2019) Impact of chemical osmosis on brine imbibition and hydrocarbon recovery in liquid-rich shale reservoirs. In: SPE annual technical conference and exhibition
- van Oort E (1994) A novel technique for the investigation of drilling fluid induced borehole instability in shales. *Rock Mech Pet Eng*. pp SPE-28064-MS.
- Wang F, Pan Z (2016) Numerical simulation of chemical potential dominated fracturing fluid flowback in hydraulically fractured shale gas reservoirs. *Pet Explor Dev* 43(6):1060–1066
- Wang M et al (2019) Occurrence mechanism of lacustrine shale oil in the Paleogene Shahejie formation of Jiyang depression, Bohai Bay Basin, China. *Pet Explor Dev* 46(4):833–846
- Xu J, Zhan S, Wang W, Su Y, Wang H (2022) Molecular dynamics simulations of two-phase flow of n-alkanes with water in quartz nanopores. *Chem Eng J* 430:132800
- You L et al (2019) Mechanism of fracture damage induced by fracturing fluid flowback in shale gas reservoirs. *Nat Gas Ind B* 6(4):366–373
- Yuan Y, Rezaee R, Zou J, Liu K (2021) Pore-scale study of the wetting behavior in shale, isolated kerogen, and pure clay. *Energy Fuels* 35(22):18459–18466
- Yuliang S, Li Z, Shiyuan Z, Li D, Sheng G (2021) Correction for capillary pressure influence on relative permeability by combining modified black oil model and genetic algorithm. *J Petrol Sci Eng* 204:108762
- Zhao W et al (2020) Types and resource potential of continental shale oil in China and its boundary with tight oil. *Pet Explor Dev* 47(1):1–11

- Zhao X et al (2021) Enrichment theory, exploration technology and prospects of shale oil in lacustrine facieszone of deep basin; a case study of the Paleogene in Huanghua depression. Bohai Bay Basin Acta Petrolei Sinica 42(02):143–162
- Zheng S and Sharma MM (2020) A comparison of hydraulic fracture propagation and well productivity using different energized fracturing fluids. In: 54th U.S. rock mechanics/geomechanics symposium
- Zhou D, Jia L, Kamath J, Kavscek AR (2002) Scaling of counter-current imbibition processes in low-permeability porous media. J Petrol Sci Eng 33:61–74
- Zhou Z, Abass H, Li X, Bearinger D, Frank W (2016) Mechanisms of imbibition during hydraulic fracturing in shale formations. J Petrol Sci Eng 141:125–132
- Zhou Z, Li X, Teklu TW (2021) A critical review of osmosis-associated imbibition in unconventional formations. Energies 14(4):835

Publisher's Note Springer Nature remains neutral with regard to jurisdictional claims in published maps and institutional affiliations.